Journal of Ceramic Processing Research. Vol. 20, No. 3, pp. 211~215 (2019)
(Received 15 November 2018, Received in revised form 17 January 2019, Accepted 9 May 2019)

J O U R N A L O F
Ceramic Processing Research

Scintillation and photoluminescence properties of Pr-doped $CaHfO_3$ crystals

Hiroyuki Fukushima*, Daisuke Nakauchi, Noriaki Kawaguchi and Takayuki Yanagida
Devision of Materials Science, Nara Institute of Science and Technology, 8916-5 Takayama-cho, Ikoma, Nara 630-0192, Japan

Pr-doped $CaHfO_3$ bulk crystals were synthesized by the floating zone method, and the luminescence properties were investigated. We confirmed that all the samples have a single phase of $CaHO_3$ by XRD measurement. The undoped sample indicate a broad emission around 440 nm and fast decay time constant due to the host while the Pr-doped samples show sharp peaks and slow decay time constants due to the 4f-4f transitions of Pr^{3+}. By Pr-doping, the afterglow level became worse than that of the undoped one while the dense Pr-doping can suppress the afterglow.

Key words: Scintillator, Photoluminescence, $CaHfO_3$, Pr-doped, Afterglow.

Introduction

Scintillator materials emit numerous photons when absorbing a high energy ionizing radiation such as gamma- and X-rays, and the application fields are positron emission tomography (PET) [1, 2], security [3], high energy physics [4] and well-logging [5]. In these application, scintillators are combined with a photo detector such as photodiode and photomultiplier. Almost commercial scintillators are doped with Ce^{3+}, and common materials are Gd_2SiO_5 [6], $Y_3Al_5O_{12}$ [7] and Lu_2SiO_5 [8]. In addition to Ce-doped scintillators, Pr-doped scintillation materials such as Pr-doped $Lu_3Al_5O_{12}$ with 5d-4f transitions [9] and Pr-doped Gd_2O_2S [10] with 4f-4f transitions also show good scintillation properties. Pr-doped $Lu_3Al_5O_{12}$ and Gd_2O_2S are utilized for photon counting type devices such as PET and integration type detector such as X-ray computed tomography (X-ray CT) due to its decay time, respectively.

Hafnium-based oxide materials such as MHfO$_3$ (M = Ca, Sr or Ba) are one of the attractive candidates for gamma- and X-ray attenuation due to its high density and high effective atomic number [11, 12]. $SrHfO_3$ have been reported with relatively high scintillation light yield (5000 photons/MeV) and fast decay time [12], and the high density and the high effective atomic number of 7.60 g/cm^3 and 63.10, respectively, are attractive for high energy photon detection. $CaHfO_3$ also has the high density (6.95 g/cm^3) and the high effective atomic number (65.15), and previous reports have shown interesting properties [13, 14]. However, synthesis of the MHfO$_3$ bulk crystal using typical crystal growth methods is extremely difficult due to its high melting temperature. Hence, almost reports of MHfO$_3$ are powder form synthesized by the typical solid state reaction [15-17]. Recently, we synthesized materials with a high melting temperature by using xenon arc lamp floating zone (FZ) furnace, and the properties were investigated [18].

In the present study, Pr-doped $CaHfO_3$ crystals were synthesized by FZ method, and the photoluminescence (PL) and scintillation properties were evaluated. Almost applications require scintillator materials in bulk form because of the detection efficiency simply depends on the volume of sensor materials. Hence, applications of scintillators in a powder form are quite limited. Up to now, Pr-doped $CaHfO_3$ have been reported only in a powder form [19], and there is a room for study in the bulk crystalline Pr-doped $CaHfO_3$. This study reports the properties of Pr-doped $CaHfO_3$ at the first time as far as we know.

Experimental

$CaHfO_3$ crystals were synthesized by FZ furnace using xenon arc lamp (Crystal Systems Corporation, FZ-T-12000-X-VPO-PC-YH) [18]. The concentrations of Pr were 0, 0.1, 1.0 and 3.0 % with respect to Ca in each sample. HfO_2 (99.95 %, Furuuchi Chemical), CaO (99.99 %, Furuuchi Chemical) and Pr_6O_{11} (99.9 %, Furuuchi Chemical) powders were used as a starting materials. First, measured powders were mixed homogeneously, and then the substance was loaded in a balloon to form a cylindrical rod using hydrostatic pressure. The rod was calcined at 1400 °C for 8 h in air. Finally, the crystal was synthesized into the FZ furnace, and the pull-down rate and the rotation rate were 30 mm/h and 3 rpm, respectively. The powder X-ray diffraction (XRD) patterns with a diffractometer (Rigaku, MiniFlex600) equipped a CuKα micro X-ray

*Corresponding author:
Tel : +81-743-72-6144
Fax: +81-743-72-6147
E-mail: fukushima.hiroyuki.ex8@ms.naist.jp

tube (40 kV and 15 mA) in the range of $2\theta = 10 - 80^{o}$.

Quantaurus-QY (Hamamatsu Photonics, C11347) was utilized to measure the PL excitation (PLE) and emission spectra as well as PL quantum yield (QY). Quantaurus-τ (Hamamatsu Photonics, C11367) was used to evaluate the PL decay curves. The undoped and Pr-doped samples under excitation 340 nm were monitored at 440 and 500 nm, respectively.

The X-ray-induced scintillation spectra were measured using the X-ray generator (Spellman, XRB80N100/CB) [20]. The X-ray tube was supplied with 80 kV and 1.2 mA as a bias voltage and a tube current, respectively. The scintillation light was measured using the spectrometer (Andor, DU-420-BU2 CCD with Shamrock SR163 monochromator) through an optical fiber of 2 m. A Peltier module cooled the CCD to 188 K. The X-ray-induced scintillation decay curves and afterglow curves were measured by our original setup [21]. The photomultiplier tube (PMT), which has the sensitive spectral range from 160 to 650 nm was utilized to detect photons. The decay time constant (τ) was deduced by the least-square fitting with sum of exponential decay functions for both the PL and X-ray-induced scintillation decay curves.

Results and Discussion

Fig. 1 shows a photograph of the undoped and Pr-doped $CaHfO_3$ crystals synthesized by the FZ method using xenon arc lamp. The undoped and 0.3 % Pr-doped samples are colorless and translucent while the 1.0 and 3.0% Pr-doped samples are green opaque. The diameter and length of the samples are 4-5 and around 2 mm, respectively. The samples as shown picture 1 were used for evaluations of luminescence properties.

Fig. 2 shows powder XRD patterns of all samples. All of the observed peaks were matched with the orthorhombic phase of $CaHfO_3$ reported previously [14]. Hence, we confirmed that the grown crystals have a single phase of $CaHfO_3$ which belongs to the *Pnma* space group of the orthorhombic crystal system [22].

Fig. 3 shows PLE-PL contour plots of the undoped and 0.3% Pr-doped samples. The PL spectral shape is

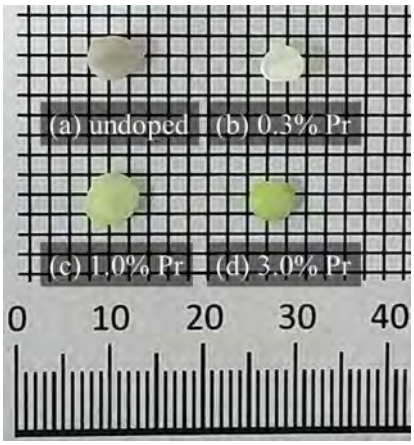

Fig. 1. Photograph of (a) undoped and (b) to (d) Pr-doped $CaHfO_3$ crystals.

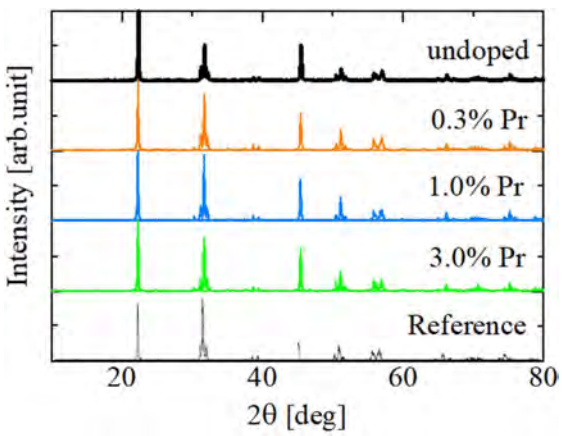

Fig. 2. Powder XRD patters of the samples.

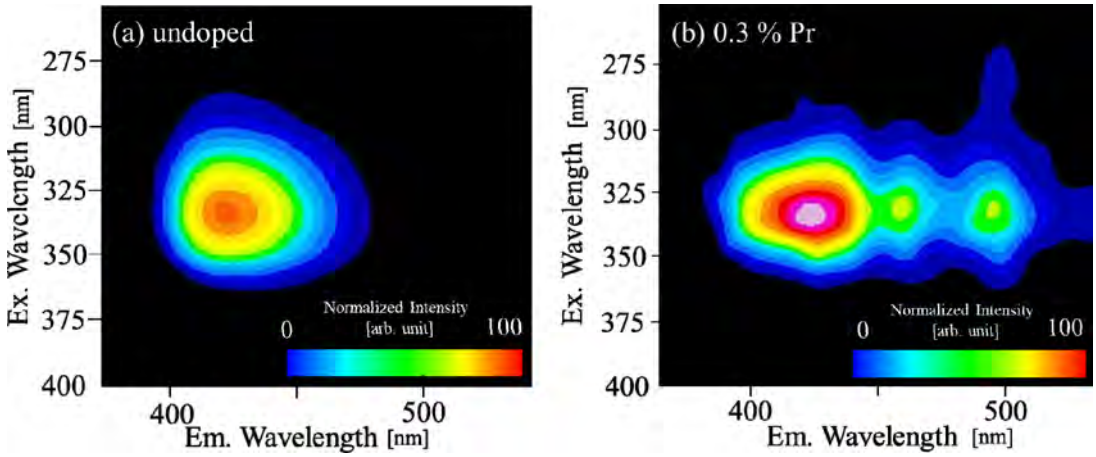

Fig. 3. PLE-PL contour plots of (a) undoped and (b) 0.3% Pr-doped $CaHfO_3$ samples. Horizontal axis shows emission wavelength (Em.), and vertical axis appears excitation wavelength (Ex.).

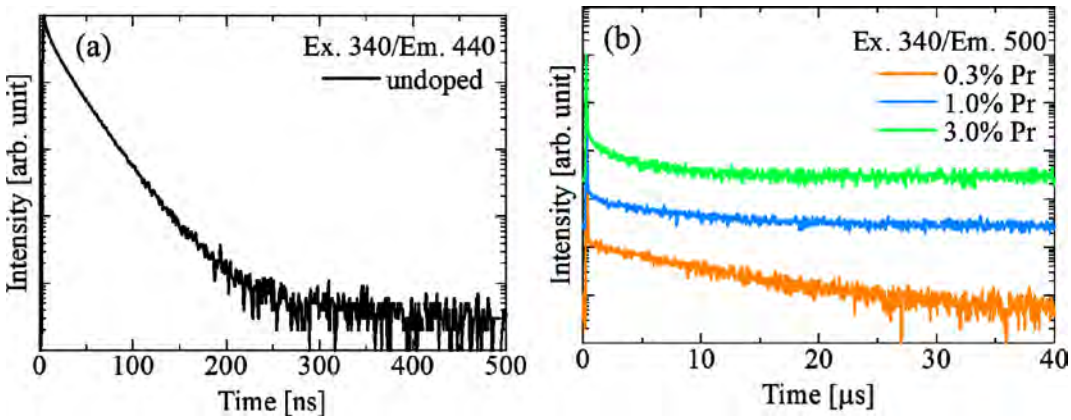

Fig. 4. PL decay curves of (a) undoped and (b) Pr-doped $CaHfO_3$ crystals under excitation at 340 nm monitored at 440 and 500 nm, respectively.

different between the undoped and the Pr-doped samples. The other two samples (Pr 1.0 and 3.0 %) showed similar spectral shape although the intensity was weaker than that of the 0.3% doped sample. The 0.3 % Pr-doped sample shows a similar broad emission band peaking at 420~440 nm with that of the undoped sample in addition to the typical luminescence features of the 4f-4f transitions of Pr^{3+} at 460 and 490 nm. The internal PL *QY* of the undoped and 0.3, 1.0 and 3.0 % Pr-doped samples are 6.3, 6.8, 1.6 and 1.4 %, respectively. The internal PL *QY* of Pr-doped $CaHfO_3$ crystals was evaluated at the first time as far as we know.

Fig. 4 shows PL decay curves of the undoped and Pr-doped samples under excitation 340 nm monitored at 440 and 500 nm, respectively. The monitoring wavelengths were determined by the PLE-PL contour graph. Table 1 lists the PL decay constants of the samples. The decay curve of the undoped sample is approximated by a sum of two exponential decay components. The first component is an instrumental response function, and the second component (τ_1) of the undoped sample would be originated from defects which were also observed in our recent report [23]. The Pr-doped samples have one exponential decay component if we neglect the spike-like component due to the instrumental response. The component (τ_1) of the Pr-doped samples show slow decay times in several μs, as summarized in Table 1. Although we could not find past literatures on decay times of Pr-doped $CaHfO_3$, the observed decay times were typical values of 4f-4f transitions of Pr^{3+}. In general, the decay times become faster owing to increment of doping concentrations, and the decay time of the Pr-doped samples becomes fast as the Pr concentration densely.

Table 1. PL decay time constant of undoped and Pr-doped $CaHfO_3$ crystals.

Sample	τ_1
undoped	25.4 ns
0.3% Pr	8.5 μs
1.0% Pr	6.1 μs
3.0% Pr	2.9 μs

Fig. 5 shows X-ray-induced scintillation spectra of Pr-doped samples. The emission peak wavelength of the undoped sample was almost the same with PL emission. The Pr-doped samples show sharp emission peaks due to the 4f-4f transitions of Pr^{3+} around 510 ($^3P_0 \rightarrow {}^3H_4$), 550 ($^3P_0 \rightarrow {}^3H_5$), 630 ($^3P_0 \rightarrow {}^3H_6$) and 660 ($^3P_0 \rightarrow {}^3F_2$). The decrease of the emission intensity and the red-shift of the peak position in higher Pr concentration were observed, and the reason was ascribed to the self-absorption of Pr^{3+} 4f-4f transition. Emission due to 5d-4f transition of Pr^{3+} was not observed in our samples. Previously, the detection of the emission from 5d-4f transition of Pr^{3+} around 300 nm was reported in Pr-doped $CaHfO_3$ [19], although decay time was not presented [19]. In addition, Pr-doped $BaHfO_3$ which had the same crystalline structure and similar chemical composition did not show d-f emission while the excitation to 5d states were observed [24]. The UV emission reported in the past work [24] was concluded as the host luminescence of

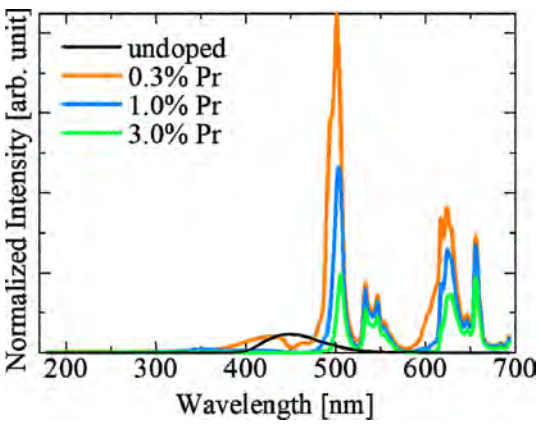

Fig. 5. X-ray-induced scintillation spectra of undoped and Pr-doped $CaHfO_3$ crystals.

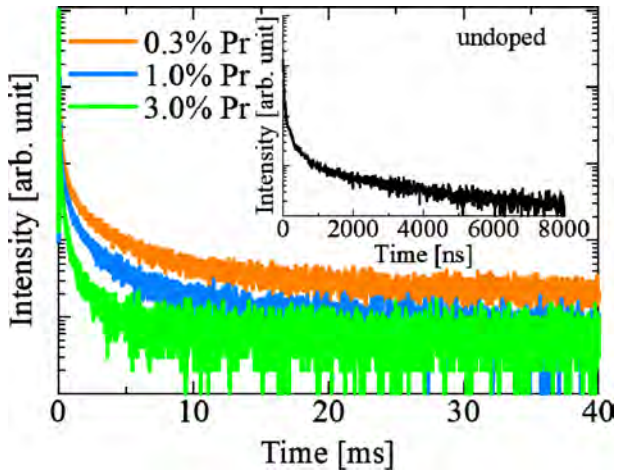

Fig. 6. X-ray-induced scintillation decay curves of undoped (inset) and Pr-doped $CaHfO_3$ crystals.

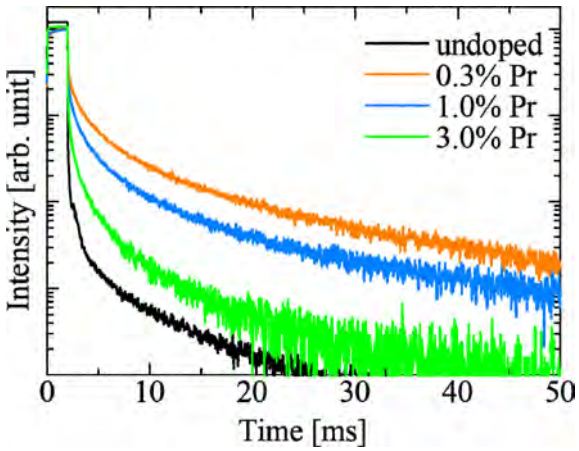

Fig. 7. Afterglow curves of undoped and Pr-doped $CaHfO_3$ crystals after 2 ms X-ray irradiation.

Table 2. X-ray-induced scintillation decay time constant and afterglow level of undoped and Pr-doped $CaHfO_3$ samples.

Sample	τ_1	τ_2	Afterglow Level [ppm]
undoped	345 ns	-	98
0.3% Pr	243 μs	3348 μs	7687
1.0% Pr	163 μs	2424 μs	3492
3.0% Pr	96 μs	945 μs	228

$BaHfO_3$. Up to now, the number of studies on Pr-doped $MHfO_3$ is limited, and further investigation is required to conclude whether d-f transition of Pr^{3+} is possible or not.

Fig. 6 demonstrates the X-ray-induced scintillation decay curves of the undoped and Pr-doped samples. The decay curve of the undoped sample is approximated by a sum of two exponential decay components. The first component of the undoped and Pr-doped samples is an instrumental response function in this time range, and the second component (τ_1) of the undoped sample would be defects origin, as discussed earlier [23]. The decay curves of the Pr-doped samples are approximated by a sum of three exponential decay components. The second (τ_1) and third (τ_2) components of the Pr-doped samples would be due to the 4f-4f transitions of Pr^{3+}. However, the scintillation decay times were longer than PL decay times in this case. In general, the scintillation process has ionization and energy-transfer, in addition to the excitation and relaxation process at localized emission center which equals to PL emission process. Hence, the scintillation decay times are often longer than the PL decay.

Fig. 7 shows afterglow curves of the undoped and Pr-doped samples with 2 ms X-ray irradiation. The afterglow levels (A) are defined as $A = 100 \times (I_2 - I_0)/(I_1 - I_0)$, where I_0, I_1 and I_2 denote the mean signal intensity before the X-ray irradiation, the mean signal intensity during the irradiation, and the signal intensity at t = 20 ms after the X-ray irradiation, respectively. Table 2 indicates the afterglow levels among the samples. Although the afterglow level increases with Pr-doping when we compare with the undoped one, the afterglow level decrease as concentration of Pr become high.

Summary and Conclusions

The Pr-doped $CaHfO_3$ bulk crystals were synthesized by the FZ method using xenon arc lamp. XRD measurement indicates the single phase of the $CaHfO_3$. The undoped sample exhibited the emission peaking around 440 nm both in PL and scintillation spectra, while the Pr-doped samples showed some emission lines due to the 4f-4f transitions of Pr^{3+} in PL and scintillation spectra. The PL and scintillation decay curves of the undoped one show fast decay of ~ 25 ns and ~ 350 ns, respectively, while the Pr-doped ones indicate slow decay up to few ms. Although the afterglow level increases by Pr-doping, high Pr concentration can decrease the afterglow level. From the results, 0.3% Pr-doping was optimum for $CaHfO_3$ in terms of the intense emission in scintillation and high PL *QY* value.

Acknowledgement

This work was supported by Grant-in-Aid for Scientific Research A (17H01375), Scientific Research B (18H03468) and JSPS Research Fellow (17J09488) from JSPS as well as A-STEP from JST. The Cooperative Research Project of Research Institute of Electronics, Shizuoka University, Terumo Foundation for Life Sciences and Arts, Izumi Science and Technology Foundation, SEI Group CSR Foundation, The Kazuchika Okura Memorial Foundation, The Iwatani Naoji Foundation and NAIST foundation are also acknowledged.

References

1. T.K. Lewellen, Phys. Med. Biol. 53 (2008) R287-R317.
2. C.L. Melcher, J. Nucl. Med. 41 (2000) 1051-1055.
3. G. Harding, Radiat. Phys. Chem. 71 (2004) 869-881.
4. J. Chen, L. Zhang and R. Zhu, Nucl. Instruments Methods Phys. Res. Sect. A. 572 (2007) 218-224.
5. T. Yanagida, Y. Fujimoto, S. Kurosawa, K. Kamada, H. Takahashi, Y. Fukazawa, M. Nikl and V. Chani, Jpn. J Appl. Phys. 52 (2013) 076401.
6. K. Takagi and T. Fukazawa, Appl. Phys. Lett. 42 (1983) 43-45.
7. T. Yanagida, H. Takahashi, T. Ito, D. Kasama, T. Enoto, M. Sato, S. Hirakuri, M. Kokubun, K. Makishima, T. Yanagitani, H. Yagi, T. Shigeta and T. Ito, IEEE Trans. Nucl. Sci. 52 (2005) 1836-1841.
8. G. Ren, L. Qin, S. Lu and H. Li, Nucl. Instruments Methods Phys. Res. Sect. A. 531 (2004) 560-565.
9. L.M. Fraile, H. Mach, E. Picado, V. Vedia and J.M. Udías, Nucl. Instruments Methods Phys. Res. Sect. A. 713 (2013) 27-32.
10. M. Yoshida, M. Nakagawa, H. Fujii, F. Kawaguchi, H. Yamada, Y. Ito, H. Takeuchi, T. Hayakawa and Y. Tsukuda, Jpn. J. Appl. Phys. 27 (1988) L1572-L1575.
11. M. Nikl, P. Bohacek, B. Trunda, V. Jary, P. Fabeni, V. Studnicka, R. Kucerkova and A. Beitlerova, Opt. Mater. 34 (2011) 433-438.
12. E. van Loef, W.M. Higgins, J. Glodo, C. Brecher, A. Lempicki, V. Venkataramani, W.W. Moses, S.E. Derenzo and K.S. Shah, IEEE Trans. Nucl. Sci. 54 (2007) 741-743.
13. S. Lee, J. Lim and Y.S. Lee, Luminescence. (2018) 1-5.
14. Y.M. Ji, D.Y. Jiang, Z.H. Wu, T. Feng and J.L. Shi, Mater. Res. Bull. 40 (2005) 1521-1526.
15. S. Derenzo, G. Bizarri, R. Borade, E. Bourret-Courchesne, R. Boutchko, A. Canning, A. Chaudhry, Y. Eagleman, G. Gundiah, S. Hanrahan, M. Janecek and M. Weber, Nucl. Instruments Methods Phys. Res. Sect. A. 652 (2011) 247-250.
16. A. Grezer, E. Zych and L. Kpiński, Radiat. Meas. 45 (2010) 386-388.
17. Y.M. Ji, D.Y. Jiang, L.S. Qin, J.J. Chen, T. Feng, Y.K. Liao, Y.P. Xu and J.L. Shi, J. Cryst. Growth. 280 (2005) 93-98.
18. D. Nakauchi, G. Okada, N. Kawaguchi and T. Yanagida Jpn. J. Appl. Phys. 57 (2018) 100307.
19. W. Jia, D. Jia, T. Rodriguez, Y. Wang, H. Jiang and K. Li, J. Lumin. 122-123 (2007) 55-57.
20. T. Yanagida, K. Kamada, Y. Fujimoto, H. Yagi and T. Yanagitani, Opt. Mater. 35 (2013) 2480-2485.
21. T. Yanagida, Y. Fujimoto, T. Ito, K. Uchiyama and K. Mori, Appl. Phys. Express. 7 (2014) 062401.
22. A. Feteira, D.C. Sinclair, K.Z. Rajab and M.T. Lanagan, J. Am. Ceram. Soc. 91 (2008) 893-901.
23. H. Fukushima, D. Nakauchi, G. Okada, N. Kawaguchi and T. Yanagida, J. Mater. Sci.Mater. Electron. (2018).
24. I.E. Seferis, K. Fiaczyk, D. Spassky, E. Feldbach, I. Romet, M. Kirm and E. Zych, J. Lumin. 189 (2017) 148-152.